Observation of exchange-scattering effects in cadmium $(e,2e)$ energy spectra

N. L. S. Martin,[1] R. P. Bauman,[1] and M. Wilson[2]
[1]*Department of Physics and Astronomy, University of Kentucky, Lexington, Kentucky 40506-0055*
[2]*Physics Department, Royal Holloway, University of London, Egham, Surrey TW20 0EX, United Kingdom*
(Received 2 September 1997)

Cadmium $(e,2e)$ energy spectra have been measured which show the effects of electron impact exchange processes at large scattering angles. As the scattering angle is increased from 2° to 15° the relative peak intensities of the $^3P_1$ and $^1P_1$ $4d^9 5s^2 5p$ autoionizing resonances change by a factor of 3. A semiempirical model is presented which seeks to parametrize all the data in terms of a single constant.
[S1050-2947(98)02103-9]

PACS number(s): 34.80.Dp, 32.80.Dz

I. INTRODUCTION

At high incident electron energy, the $(e,2e)$ technique can be used to simulate photoionization [1]; in the small momentum-transfer (K) limit, $(e,2e)$ spectra are dominated by dipole processes and closely mimic photoelectron spectra. At intermediate energies, where nondipole effects, although small, are noticeable, the dominant dipole term may be isolated. Thus Ref. [2] used the $(e,2e)$ method to measure the Cd β parameter in the $4d^9 5s^2 5p$ autoionizing region, and Ref. [3] directly compared high resolution $(e,2e)$ spectra with their Cd photoelectron counterparts.

This technique manipulates the $(e,2e)$ data in a manner suggested by a partial wave expansion of the ejected-electron wave function within the plane-wave Born approximation (PWBA): (a) for $K \ll 1$ the series can be terminated at $l = 2$; and (b) the sum of $(e,2e)$ spectra for ejected-electron directions 180° apart eliminates interference cross-terms, leaving an almost pure dipole spectrum [4]. Thus it is possible to extend the ''dipole approximation'' into the intermediate energy region, provided that K remains small.

For $(e,2e)$ experiments carried out at larger K, this good agreement with photoelectron data is expected to break down for a number of reasons. In this work we isolate one of these, the effect of electron exchange scattering on the $(e,2e)$ spectra of autoionizing levels. In our analysis we also have to take into account the fact that additional multipoles become significant, and their effect is not totally eliminated by the spectral addition technique described above. A third possible effect is that the symmetry axis given in the PWBA by the momentum-transfer direction, and used in the $(e,2e)$ analysis as equivalent to the photon polarization direction, loses its special status as the $\Delta M = 0$ selection rule begins to break down. In scattering theory terms this is the point at which the distorted-wave Born approximation (DWBA) treatment begins to differ from the plane-wave treatment. A quantitative analysis based on the DWBA is beyond the scope of the present work; however, we find that it is possible to explain the gross features of our $(e,2e)$ data in terms of the PWBA modified to include exchange scattering.

The earliest Cd measurements that investigated these effects were carried out at a fixed incident electron energy, with the momentum transfer varied by varying the scattering angle [5]; $(e,2e)$ ejected-electron angular distributions were obtained for the $4d^9 5s^2 5p\ ^1P_1$ autoionizing resonance, for an incident energy of 150 eV and scattering angles up to 24°. The results were compared with (dipole only) DWBA calculations that did not include exchange [6]. This analysis, however, in terms of incoherent sums of dipole and nondipole terms, is now known to be inappropriate in the light of recent experiments [4]. These measured $(e,2e)$ ejected-electron spectra over the entire $4d^9 5s^2 5p$ region, rather than angular distributions only in the $4d^9 5s^2 5p\ ^1P_1$ peak, and, even though these were carried out at small scattering angles, they demonstrated that it is necessary to consider interference cross-terms between dipole and nondipole terms in the analysis of coplanar $(e,2e)$ measurements restricted to only one side of the scattering axis (i.e., either the binary or the recoil side) [7].

We have therefore carried out a comprehensive set of measurements of $(e,2e)$ spectra in the $4d^9 5s^2 5p$ autoionizing region for scattering angles up to 20° corresponding to the momentum transfer range $0.2 \rightarrow 1$ a.u. A full description of these experiments will be published in a later paper. Here we report the observation of a striking variation in the relative intensity of two $4d^9 5s^2 5p$ dipole resonances, and its interpretation in terms of exchange scattering. Section II summarizes the theory with which the effects are analyzed, Sec. III gives experimental details, and Secs. IV and V give the experimental results and the conclusions.

II. THEORY

The ground state of cadmium is $4d^{10} 5s^2\ ^1S_0$, with photoionization via a dipole process resulting in the population of the $5sEp\ ^{1,3}P_1$ continua; only ionization into the ground ionic state $5s\ ^2S_{1/2}$ is of interest here. For ejected electrons in the energy range $2.5 \rightarrow 4.5$ eV, this process is dominated by the autoionizing configuration $4d^9 5s^2 5p$, which gives rise to three $J = 1$ levels, $\rho = 1$, 2, and 3, with energies $E_\rho = 3.07$, 3.81, and 3.94 eV, above the ground-state ion energy of 8.99 eV [8,9]. Because of the large spin-orbit energy of the $4d$ electron, each level is an admixture of $^1P_1$, $^3P_1$, and $^3D_1$ basis states $t = 1$, 2, and 3, respectively. The composition of each level is described by mixing coefficients $\mu_{\rho t}$.

Thus each sublevel may be represented by

$$|\rho\rangle = \sum_t \mu_{\rho t} |t\rangle. \tag{1}$$

Only the $^1P_1$ component of each level takes part in the photoexcitation of each level, because of the selection rules $\Delta J = 1$ and $\Delta S = 0$. Thus the photoabsorption *amplitude* associated with each level ρ is proportional to $\mu_{\rho 1}$ multiplied by the $4d \rightarrow 5p$ amplitude. The photoabsorption cross-section will be proportional to the square of these quantities; this was quantitatively verified in Ref. [10], which demonstrated that the photoabsorption intensity associated with each of the three levels may be well described by the independent-particle model using a single configuration. (The presence of other, $5pnl$ autoionizing configurations only affects details of the line shape but has no effect on the overall intensity, [11].) The photoelectron angular distribution is a more complex phenomenon to model than the photoabsorption cross section since both $^1P_1$ and $^3P_1$ discrete components interact with the $^1P_1$ and $^3P_1$ $5sEp$ continua. However, spectra equivalent to absorption spectra may be obtained from measurements taken at an angle $\theta = 54.7°$ with respect to the polarization direction [12], the ''magic angle'' for which the second-order Legendre polynomial $P_2(\cos\theta)$ vanishes.

For linearly polarized light it is convenient to take the polarization direction as the quantization axis, in which case there is the additional selection rule $\Delta M_J = 0$. For electron scattering, in the PWBA without exchange, the selection rules $\Delta M_J = 0$ and $\Delta S = 0$ also apply if the momentum-transfer direction is taken as the quantization axis. In particular, in a multipole expansion of the scattering amplitude, the relative dipole terms for the three $4d^9 5s^2 5p$ levels will again be proportional to $\mu_{\rho 1}$, this time multiplied by a PWBA $4d \rightarrow 5p$ amplitude $f(K)$ common to all three levels,

$$\mathcal{A}(E_\rho) \propto \mu_{\rho 1} f(K). \tag{2}$$

Thus, within the PWBA without exchange, the relative intensities of the three levels is independent of magnitude K of the momentum transfer, and hence the $^3P_1/^1P_1$ intensity ratio should be independent of the scattering angle.

When electron exchange is allowed during the scattering process, the selection rule on the spin change of the target is $\Delta S = 0, \pm 1$. The intensity of the three $4d^9 5s^2 5p$ levels then depends on transitions to both the $^1P_1$ and $^3P_1$ basis states. The amplitude for each level is a coherent summation of the $^1P_1$ and $^3P_1$ amplitudes. There is thus the possibility of destructive or constructive interference which can change the relative intensity of the $4d^9 5s^2 5p$ levels. The formalism of exchange scattering for complex atoms has been given by a number of authors [13–15]. Rather than adapt these to the present case, we found it more straightforward to derive our own expression in terms of LS-coupled basis states.

We wish to find the form of the matrix element, due to electron impact, mediated by some general interaction $\hat{T}$, for the transition $l \rightarrow l'$ of an electron in a subshell nl containing w electrons where $w \leqslant 3(2l+1)$, and the initial and final states are LS coupled:

$$(l^w)^{2S+1}L_J + e(m_\sigma) \rightarrow \{[l^{w-1}(^{2S_C+1}L_C)]l'\}^{2S'+1}L'_{J'} + e(m'_\sigma). \tag{3}$$

The incident electron is taken to be polarized with initial spin component m_σ and final spin component m'_σ. Although spin-independent interactions are assumed, the use of fully antisymmetric wave functions to describe the system of $w+1$ electrons allows for exchange interactions with $m'_\sigma \neq m_\sigma$. We assume an LS-coupled frozen core $(l^{w-1})L_C S_C$, which needs to be uncoupled from the jumping electron $l \rightarrow l'$ on both sides of the matrix element. In the spirit of the frozen-core approximation, we neglect a small term due to exchange between the frozen core and the incident electron accompanied by promotion of the active electron.

We then find

$$\begin{aligned}
&\langle \Psi_{l^w\ 1l'}[(L_C S_C)L'S'J'M'_J]\psi_f(m'_\sigma)|A^\dagger \hat{T} A|\Psi_{l^w}(LSJM_J)\psi_i(m_\sigma)\rangle \\
&= \sqrt{w}(l^{w-1}L_C S_C|\}l^w LS) \sum_{M_L M_S} \sum_{M_{L_C} m_l} \sum_{M_{S_C} m_s} C^{LSJ}_{M_L M_S M_J} C^{L_C l L}_{M_{L_C} m_l M_L} C^{S_C (1/2) S}_{M_{S_C} m_s M_S} \\
&\times \sum_{M'_L M'_S} \sum_{M_{L_C} m'_l} \sum_{M_{S_C} m'_s} C^{L'S'J'}_{M'_L M'_S M'_J} C^{L_C l' L'}_{M_{L_C} m'_l M_L} C^{S_C (1/2) S'}_{M_{S_C} m'_s M_S} [f_{lm_l \rightarrow l'm'_l} \delta_{m_\sigma m'_\sigma} \delta_{m_s m'_s} - g_{lm_l \rightarrow l'm'_l} \delta_{m_\sigma m'_s} \delta_{m_s m'_\sigma}].
\end{aligned} \tag{4}$$

Here upper case Ψ indicates an antisymmetrized target wave function, and lower case ψ represents the nonantisymmetrized projectile, A is the special operator that antisymmetrizes the product $\Psi\psi$ for the $(w+1)$ electron system, $C^{j_1 j_2 j_3}_{m_1 m_2 m_3}$ is a Clebsch-Gordon coefficient, and $(l^{w-1}L_C S_C|\}l^w LS)$ is a coefficient of fractional parentage [16]. As pointed out by Bonham [15], different authors use different definitions for the direct and exchange amplitudes. Here the direct $f_{lm_l \rightarrow l'm'_l}$ and exchange $g_{lm_l \rightarrow l'm'_l}$, amplitudes are defined in terms of single-particle transitions. Thus Eq. (4), which is the result of extensive summation over antisymmetric permutations within the subshell, has a remarkably hydrogenlike form. A similar observation was made by Rudge [13] who used $LM_L SM_S$ coupling, rather than the more general $LSJM_J$ coupling used here. In principle, some of the summations could be carried out analyti-

TABLE I. Cadmium $4d^9 5s^2 5p\ J=1$ autoionizing level energies [above the 8.99-eV ionization potential (IP)], widths, and $^1P_1$ and $^3P_1$ eigenvector compositions. The $^3D_1$ component plays no part in either excitation or autoionization, and is not shown. The labels ρ and t refer to Eq. (1).

	Energy (eV)	Width (eV)	Component ($\mu_{\rho t}$)	
			$t=1$ $^1P_1$	2 $^3P_1$
$\rho=1$	3.07	0.041	−0.3479	−0.9101
2	3.81	0.140	+0.9294	−0.3663
3	3.94	0.003	+0.1224	+0.1935

cally and the result partially expressed in terms of $6-j$ coefficients [16], but we find that a simple and fast computer program may be easily written in terms of the Clebsch-Gordon coefficients.

An extension of the PWBA to include exchange is due to Bonham [17] and Ochkur [18]. The result, expressed in terms of the incident projectile momentum k and momentum transfer K, is

$$g=\frac{K^2}{k^2}\,f. \tag{5}$$

This approximation is expected to work best when exchange effects are small [17]. In the analysis of our experimental data, where exchange effects are large, we have therefore adopted the semiempirical relationship

$$g=C\,\frac{K^2}{k^2}\,f, \tag{6}$$

where C is a constant, independent of K and the scattering angle, that will be determined by obtaining a reasonable fit to all the experimental data. The amplitudes, in the PWBA including exchange, of the $4d^9 5s^2 5p\ J=1$ autoionizing levels are then given by

$$\mathcal{A}(E_\rho)\propto\left[\mu_{\rho 1}\left(1-\frac{1}{2}\,C\,\frac{K^2}{k^2}\right)+\mu_{\rho 2}\,\frac{1}{2}\,C\,\frac{K^2}{k^2}\right]f(K), \tag{7}$$

where Eq. (4) was used to evaluate the factors $f-\frac{1}{2}g$ for $^1P_1$ and $+\frac{1}{2}g$ for $^3P_1$. Table I gives the relevant properties of these three levels, as given by the analysis of Ref. [10]. It can be seen that the third level at 3.94 eV, which is of mainly $^3D_1$ character, is very narrow and very weakly excited. Thus its contribution to the overall line profile, particularly for the $(e,2e)$ experiments with limited energy resolution, is very small (but is included in our full calculations). Using the values from the table for the remaining levels gives

$$\mathcal{A}(3.07)\propto-0.3479\left(1+(0.8080)C\,\frac{K^2}{k^2}\right)f(K) \tag{8a}$$

and

$$\mathcal{A}(3.81)\propto+0.9294\left(1-(0.6971)C\,\frac{K^2}{k^2}\right)f(K). \tag{8b}$$

The sign of C determines in which of the two levels destructive interference occurs; constructive interference then always occurs in the other. [This follows from the fact that the $(\rho=1,2;\ t=1,2)$ submatrix is an approximately orthogonal matrix.] The ratio of the intensity of the two levels is strongly dependent on exchange effects:

$$\left(\frac{\mathcal{A}(3.07)}{\mathcal{A}(3.81)}\right)^2=0.140\left(1+\frac{1.505X}{1-0.697X}\right)^2, \tag{9a}$$

where

$$X=C\,\frac{K^2}{k^2}. \tag{9b}$$

These relationships show that the relative intensity of these two levels should provide an absolute determination of exchange effects. In fact the presence of other multipole amplitudes for the nonresonant ionization $5s^2\rightarrow 5sEl$ needs to be taken into account. In analyzing the data we have therefore carried out a full calculation, as described in Ref. [4], but for $l=0\rightarrow 6$. These calculations are for summed $(e,2e)$ spectra taken 180° apart; this manipulation eliminates cross-terms of different parity [4], and therefore helps to emphasize the dominant dipole term. We incorporated the phase correction for $l=0$ found from this earlier work; however, we find that the summed spectrum is almost independent of this correction since the most important cross-term, $(l=0)(l=4)$, is very small (all $l=2$ terms vanish at the magic angle). Details of the *ab initio* calculation of the PWBA amplitudes $f_{5s\rightarrow El}$ and $f_{4d\rightarrow 5p}$ will be given in a later publication. Evaluation of Eq. (4) shows that for $J=L=l$ the $5sEl\ ^1L_J$ continuum amplitude f is replaced by $f-\frac{1}{2}g$, and the ^3L_J continuum amplitude (for $l>0$) is proportional to $+\frac{1}{2}g$, as was the case for the $4d^9 5s^2 5p$ singlet and triplet basis states. The exchange amplitude g we again approximated by Eq. (6); the empirical constant C is taken to have the same value for all multipoles of both resonant and nonresonant processes.

III. EXPERIMENT

The coplanar $(e,2e)$ spectrometer has been described in detail elsewhere [4,19]. It consists of four main components: an electron gun, a metal-vapor atomic beam oven, a scattered electron spectrometer, and an ejected-electron spectrometer. The electron gun is recessed in a side arm of the vacuum chamber, which enables the ejected-electron spectrometer to be positioned on both sides of the electron-beam axis. Thus $(e,2e)$ spectra for two ejected-electron angles 180° apart may be taken in a single experimental run at the same value of θ_{sc}. Auger peaks in the noncoincident ejected-electron spectrum are used for energy calibration and alignment, and intensity normalization; details are given in Ref. [20].

The ejected-electron detector contains a resistive anode-type position-sensitive detector; this system enables useful count rates to be obtained at an energy resolution of 40 meV. During an experiment, energies and angles are scanned repetitively to minimize the effect of any drift in, for example, the electron-beam intensity. Run times of about ten days are

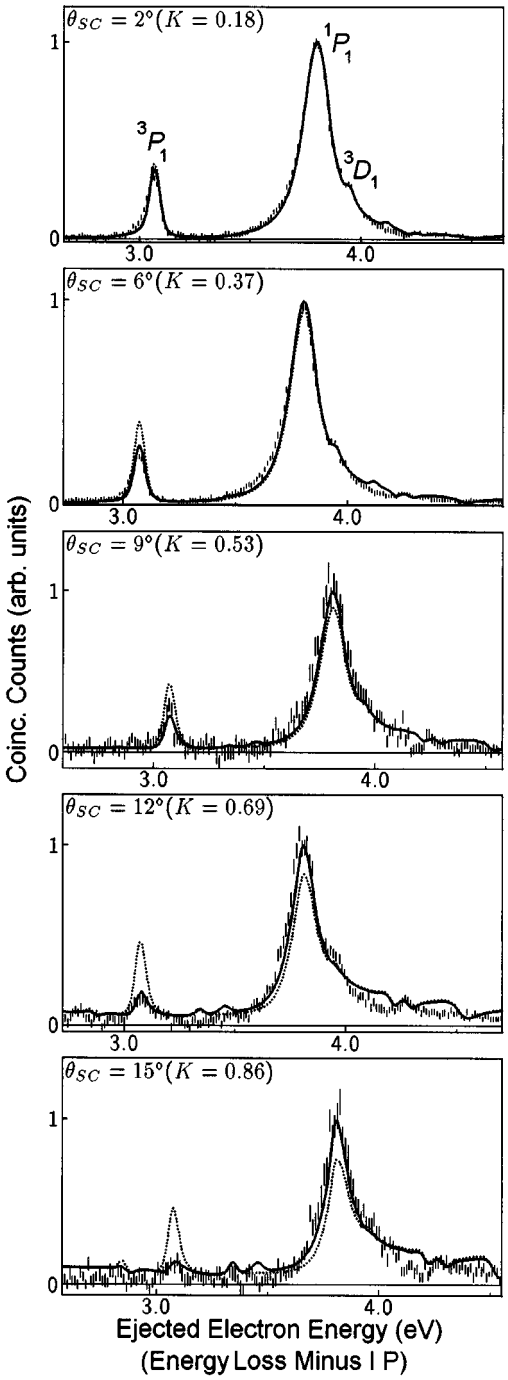

FIG. 1. Experimental magic angle $(e,2e)$ sum spectra of Cd for different scattering angles θ_{SC}. The vertical bars represent the statistical uncertainties. The three $4d^9 5s^2 5p$ autoionizing resonances are labelled. The solid and dotted lines are PWBA calculations with and without exchange, respectively. The exchange calculations have $C=-10$ (see text) and are normalized to the experiments at 3.81 eV.

necessary in order to acquire an $(e,2e)$ spectral pair with adequate statistics.

IV. RESULTS AND DISCUSSION

Coplanar $(e,2e)$ spectra in Cd were obtained with an incident electron-beam energy of 150 eV, scattering angles

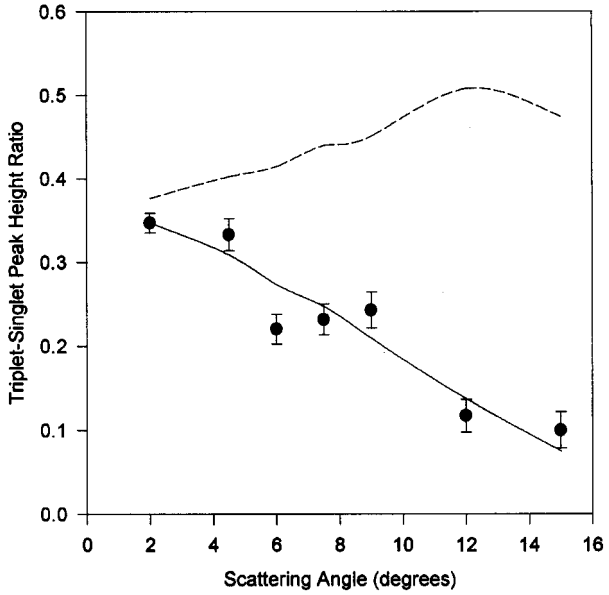

FIG. 2. Ratio of $^3P_1$ and $^1P_1$ peak heights of magic angle $(e,2e)$ sum spectra as a function of the scattering angle θ_{SC}. The vertical bars represent the estimated uncertainty of the experimental values. The solid and dashed lines are absolute PWBA calculations with and without exchange. The exchange calculations have $C=-10$ (see text).

from $\theta_{sc}=2°$ to 15°, such that $K\approx 0.2\rightarrow 0.9$ a.u., and ejected-electron energies $E\approx 2.5\rightarrow 5$ eV. Each experiment was carried out at a pair of ejected-electron angles θ_{ej} and $\theta_{ej}+180°$ which were the ''magic angle'' away from the momentum-transfer direction θ_K given by $\theta=\theta_K-\theta_{ej}\pm\cos^{-1}(1/\sqrt{3})\approx 54.7(+180)°$.

Figure 1 shows the sum of the spectral pairs for a representative set of the experimental results. The experimental energy resolution for all spectra corresponds to a Gaussian instrument function of full width at half maximum (FWHM) 40 meV. As can be clearly seen, the $^3P_1/^1P_1$ intensity ratio of the peak heights decreases rapidly with increasing scattering angle. At the smallest scattering angle the ratio is close to the photoabsorption value (corresponding to our FWHM) of about $\frac{1}{3}$. At the largest scattering angle this ratio has dropped by a factor of 3 to a value of approximately $\frac{1}{10}$. Also shown in Fig. 1 are the PWBA calculations, with and without exchange, of the summed spectra. The exchange calculation has been normalized to the experiment in the peak of the $^1P_1$ for each scattering angle; the nonexchange calculation is plotted on the same scale to show the difference between the two calculations. We find that quite good agreement between the theory with exchange and all the experiments is obtained with $C=-10$ [see Eq. (6)], i.e., exchange effects are ten times as large as, and g/f has the opposite sign to, the predictions of the Bonham-Ochkur approximation.

The $4d^9 5s^2 5p$ $J\neq 1$ levels have energies predicted by Ref. [21], and some of these are included in our calculation. The $J=3$ levels appear at about 2.8 and 3.3 eV for the largest scattering angles; a detailed analysis of these levels will appear in a later publication. The calculations also include the pure $4d^9 5s^2 5p$ $^3P_0$ level just below 3.5 eV. Although the experimental statistics preclude the observation of this level, we have incorporated it in the calculation because it

indicates the expected intensity of a pure exchange transition. A comparison of the calculated $^3P_1$ and $^3P_0$ intensities at $\theta_{sc}=15°$ then demonstrates the large effect that the interference between f and g has on the former, compared with the small absolute intensity of the later which is determined by $|g|^2$.

One prediction of the PWBA calculations appears to be verified: as the scattering angle increases, the $^1P_1$ line profile becomes more asymmetric due to a decreasing Fano q parameter [22] for dipole ionization. The near-infinite value at small scattering angles reduces to $q\approx 5$ at $\theta_{sc}=15°$.

The experiments are summarized in Fig. 2, which shows the $^3P_1/^1P_1$ peak intensity ratio for all the scattering angles investigated. The values plotted were corrected for the experimental or theoretical backgrounds of Fig. 1; uncertainties in this correction are mainly responsible for the error bars shown for the experimental data. Note that, because of interference cross-terms between different multipoles, the nonexchange calculation predicts that the ratio should not remain constant, but should increase slightly with scattering angle. The exchange calculation is in good agreement, within the experimental error bars, over the whole range of scattering angles.

V. CONCLUSIONS

$(e,2e)$ spectra in cadmium have been measured which appear to show the effects of electron-exchange scattering. These can be modeled by a simple modification to the PWBA, based upon the Bonham-Ochkur approximation. However, the fact that the exchange effects are an order of magnitude greater than predicted by the unmodified theory is somewhat puzzling. It would be interesting to see if more advanced scattering theories, such as the DWBA, can predict the correct $^3P_1/^1P_1$ intensity ratios. These theories are not restricted by the ΔM selection rules of the PWBA, and can also lead to phase differences between f and g.

ACKNOWLEDGMENTS

This work was supported by a grant from the U.S. Department of Energy, Office of Basic Energy Sciences, Division of Chemical Sciences, Fundamental Interactions Branch, under Contract No. DE-FG05-91ER14214. M.W. acknowledges the support of the EU HCM network program and the U.K. PPARC. We wish to thank M. J. Cavagnero for helpful discussions.

[1] A. Hamnett, W. Stoll, G. Branton, C. E. Brion, and M. J. Van der Wiel, J. Phys. B **9**, 945 (1976).
[2] N. L. S. Martin and D. B. Thompson, J. Phys. B **25**, 115 (1992).
[3] N. L. S. Martin, D. B. Thompson, R. P. Bauman, M. Wilson, J. Jiménez-Mier, C. D. Caldwell, and M. O. Krause, J. Phys. B **27**, 3945 (1994).
[4] N. L. S. Martin, D. B. Thompson, R. P. Bauman, and M. Wilson, Phys. Rev. A **50**, 3878 (1994).
[5] N. L. S. Martin and K. J. Ross, J. Phys. B **15**, 3959 (1982).
[6] V. V. Balashov, E. G. Berezhko, A. N. Grum-Grzhimailo, N. M. Kabachnik, and A. I. Magunov, J. Phys. B **13**, L269 (1980).
[7] N. L. S. Martin, R. P. Bauman, D. B. Thompson, M. Wilson, and K. J. Ross, J. Phys. B **29**, 4457 (1996).
[8] G. V. Marr and J. M. Austin, Proc. R. Soc. London, Ser. A **310**, 137 (1969).
[9] M. Wilson, J. Phys. B **1**, 736 (1968).
[10] N. L. S. Martin, J. Phys. B **23**, 2223 (1990).
[11] N. L. S. Martin and M. Wilson, J. Phys. B **25**, L463 (1992).
[12] J. Jimenez-Mier, C. D. Caldwell, and M. O. Krause, Phys. Rev. A **39**, 95 (1989).
[13] M. R. H. Rudge, Rev. Mod. Phys. **40**, 563 (1968).
[14] D. H. Madison and W. M. Shelton, Phys. Rev. A **7**, 499 (1973).
[15] R. A. Bonham, J. Phys. B **23**, 513 (1990).
[16] R. D. Cowan, *The Theory of Atomic Structure and Spectra* (University of California Press, Berkeley, 1981).
[17] R. A. Bonham, J. Chem. Phys. **36**, 3260 (1962).
[18] V. I. Ochkur, Zh. Eksp. Teor. Fiz. **45**, 734 (1963) [Sov. Phys. JETP **18**, 503 (1964)].
[19] N. L. S. Martin and D. B. Thompson, J. Phys. B **24**, 683 (1991).
[20] D. B. Thompson and N. L. S. Martin, J. Electron Spectrosc. Relat. Phenom. **77**, 277 (1996).
[21] N. L. S. Martin, J. Phys. B **17**, 1797 (1984).
[22] U. Fano, Phys. Rev. **124**, 1866 (1961).